PHYSICAL REVIEW D **85,** 084037 (2012)

Random tensor models in the large N limit: Uncoloring the colored tensor models

Valentin Bonzom,[1,*] Razvan Gurau,[1,†] and Vincent Rivasseau[1,2,‡]

[1]*Perimeter Institute for Theoretical Physics, 31 Caroline Street N, Ontario N2L 2Y5, Waterloo, Canada*
[2]*Laboratoire de Physique Théorique, CNRS UMR 8627, Université Paris XI, 91405 Orsay Cedex, France*

(Received 23 February 2012; published 26 April 2012)

Tensor models generalize random matrix models in yielding a theory of dynamical triangulations in arbitrary dimensions. Colored tensor models have been shown to admit a $1/N$ expansion and a continuum limit accessible analytically. In this paper we prove that these results extend to the most general tensor model for a single generic, i.e. nonsymmetric, complex tensor. Colors appear in this setting as a canonical bookkeeping device and not as a fundamental feature. In the large N limit, we exhibit a set of Virasoro constraints satisfied by the free energy and an infinite family of multicritical behaviors with entropy exponents $\gamma_m = 1 - 1/m$.

DOI: 10.1103/PhysRevD.85.084037 PACS numbers: 02.10.Ox, 04.60.Gw, 05.50.+q

I. INTRODUCTION

Matrix models are probability measures for random matrices M of size N. In physics language, they come with a matrix action $S(M)$. They can be divided in two broad categories. In the first category, that of *invariant matrix models* [1], the full action has an expansion in terms of traces of powers of M (for Hermitian, or $\mathrm{Tr}(MM^\dagger)^n$ for general M) which ensures invariance under $U(N)$ transformations. The archetypes for this category are the $\lambda\,\mathrm{Tr}M^3$ or $\lambda\,\mathrm{Tr}M^4$ models, whose actions are $S = \mathrm{Tr}M^2 + \lambda\,\mathrm{Tr}M^3$ or $S = \mathrm{Tr}M^2 + \lambda\,\mathrm{Tr}M^4$. The perturbative expansion of such models involves ribbon graphs dual to triangulated, or quadrangulated, Riemann surfaces. Hence (forgetting for a brief moment the constructive issues) these models are statistical models of random *discretized* Riemann surfaces. In the *large N* limit, planar surfaces dominate and furthermore undergo at some finite coupling a transition to *continuous* surfaces [2,3], known as the large volume, or continuum limit. Hence they provided until recently the only known example of analytically controlled geometrogenesis,[1] i.e. the emergence of continuous geometries from discrete models, although restricted to two dimensions. Moreover invariant single or multi-matrix models can also probe the critical behavior of two-dimensional statistical models on random geometries [5–8].[2]

The second category of matrix models is that of *matrix field theories*, in which the interaction is invariant, but the quadratic part of the action is not. Since invariant $\mathrm{Tr}M^n$ interactions are the matrix analogs of *local interactions* $\int \phi^n(x)$, matrix field theories are the analogs of ordinary quantum field theories, in which interactions are local but the propagator (inverse of the Laplacian or Dirac operator) is not. From this point of view invariant matrix models should be considered as *ultralocal* matrix field theories. Nonlocal propagators in field theory give birth to renormalization, hence to a flow of the couplings. Just as ϕ_4^4 is the archetype for ordinary renormalization, the archetype of matrix field theories is the Grosse-Wulkenhaar model in four dimensions,[3] or GW_4 [13]. This GW_4 model improves on the ordinary ϕ_4^4 model since it is asymptotically safe [14], hence free of the old Landau ghost problem.

Returning now to the important constructive question, let us recall that the constructive analysis of stable invariant matrix models is compatible with their $1/N$ expansion. Borel summability has been proved to hold uniformly in N in the quartic case [15]. For higher degree stable interactions a straightforward generalization of the techniques of [16] should also lead to uniform Borel-LeRoy summability of the appropriate order. The constructive analysis of matrix field theories is under way [17] and expected to lead to a full construction of the GW_4 model in the near future.

All these nice properties of matrix models stem from their $1/N$ expansion [18], which states that planar graphs (dual to the sphere) govern their large N limit.[4] Planar graphs proliferate only exponentially in their number of vertices and can be counted precisely through algebraic equations [22], as they are related to trees [23–25]. This key feature underlies all the statistical mechanics applications of the invariant models. Renormalizability and asymptotic safety in the GW_4 model also rely entirely on the dynamical analog of the $1/N$ expansion [13,14,26,27].

*vbonzom@perimeterinstitute.ca
†rgurau@perimeterinstitute.ca
‡vincent.rivasseau@gmail.com

[1]This term has appeared for the first time in [4] which is however quite different from our approach.

[2]This critical behavior on random geometry is related to the one on fixed geometry through the KPZ correspondence [9–12].

[3]The Grosse-Wulkenhaar model is a ϕ_4^{*4} model on the noncommutative Moyal space with a harmonic potential. It does not suffer from the UV/IR mixing and becomes a matrix field theory in the Moyal matrix base.

[4]Through double scaling limits one can even to some extent treat the sum over subleading terms in the $1/N$ expansion [19–21].

Indeed in such matrix field theories only planar graphs with a single external face look like matrix invariant terms at high energy, and they are also the only ones to require renormalization.

Random matrices generalize in higher dimensions to random tensors [28–30] (and [31–33] for more recent developments), whose perturbative expansion performs a sum over random higher dimensional triangulations, but until recently all nice aspects of matrix models listed above could not be generalized to tensors, as their $1/N$ expansion was missing. The situation has changed with the discovery of *colored* [34–36] rank $D \geq 3$ random tensor models.[5] These models require $D+1$ different pairs of conjugate tensors T^i, $\bar{T}^i$, equipped with a particular invariant canonical action of the type $\sum_i T^i \bar{T}^i + \lambda \prod_{i=0}^{D} T^i + \bar{\lambda} \prod_{i=0}^{D} \bar{T}^i$. Their perturbation theory supports a $1/N$ expansion [38–40], indexed by the *degree*, a positive integer which plays in higher dimensions the role of the genus but is not a topological invariant. Leading order graphs triangulate the D-dimensional sphere in any dimension [38,39]. These graphs, baptized *melonic* [41], again proliferate only exponentially, as they map to colored $(D+1)$-ary trees [41,42]. Like matrix models, these tensor models reach a continuum limit when the coupling constant approaches its critical value. The corresponding entropy exponent is $\gamma_{\text{melons}} = 1/2$ in any dimensions [41]. It is the analog of the string susceptibility exponent $\gamma_{\text{string}} = -1/2$ of the invariant matrix models for the universality class of pure $2d$ quantum gravity,

Colored random tensors [43] therefore gave the first theory of random geometries in three and more dimensions with analytically tractable geometrogenesis and the subject is rapidly expanding [44–50]. Coupling of statistical mechanical systems to these random geometries in arbitrary dimension has been done in [48,51,52], and results at all orders in $1/N$ have been established for some restricted models [53] (see also [54] for some related developments).

Obvious questions then arise. Do $1/N$ expansions also hold for uncolored models, i.e. with a single tensor? How can one build tensor models with interactions of arbitrary degree that still admit a $1/N$ expansion? What are the tensor analogs of matrix field theories?

A first important step towards answering the first two questions was taken in [42]. It was shown that integrating out all colored tensors but one in the initial colored model leads to an effective action for a single *uncolored* tensor which is a sum of effective invariant interactions whose internal structure can be unfolded in terms of colored graphs.

In the present paper we return to these questions in greater detail. As in the case of matrices, we can distinguish invariant tensor models and tensor field theories. Invariant tensor models are those considered in this paper. They correspond to tensors with both quadratic part and interactions invariant under the external tensor product $\otimes^D U(N)$. We consider the most general invariant models for a *random, complex tensor*. It is important that this tensor is generic, that is without any symmetrization or antisymmetrization of its indices. Labeling these indices then provides exactly the same combinatorial tool that colors provide in the colored models. It allows us to do the following:

(i) define their $1/N$ expansion, again organized according to the degree of the graphs;
(ii) prove it is dominated by melonic, colored graphs of spherical topology;
(iii) derive the continuum limit, whose entropy exponent is generically $\gamma_{\text{melons}} = 1/2$, thus proving the universality of this continuum phase;[6]
(iv) extract a set of Virasoro constraints which hold in the large N limit;
(v) and find multicritical points, with entropy exponents $\gamma_m = 1 - 1/m$ (for $m \geq 2$ integers), which are the same as the ones of multicritical branched polymers [48,53,55]. This is the generalization of [8] to tensors.

These are the main results of this paper, and they are direct consequences of the *universality* of tensor invariant measures first derived in [56]. We stress that universality in this context *only* means that in the large N limit the tensors are distributed on a Gaussian. However, the Gaussian itself (i.e. its covariance) is *not* universal, but depends on the coupling constants of the model. Indeed, when the large N covariance becomes critical, the continuum limit is reached. Further, tuning the couplings appropriately, multicritical behaviors are observed, just like in invariant matrix models [8].

We expect the constructive analysis of stable and symmetric invariant models not to pose any difficulty, as the necessary techniques have been in fact already developed for the quartic case [57] in the slightly different context of group field theory [58].

Tensor field theories are the analogs of matrix field theories. They have tensor invariant interactions but a Laplacian-based propagator. Such a propagator again allows a renormalization group analysis. We do not consider this second category of models further in this paper, except

[5] In $D = 2$ colors do not play the key role they play in three and more dimensions. This is because there is a natural composition rule on rank 2 tensors, namely, matrix multiplication, and a single trace invariant at order n, namely $\text{Tr}M^n$. In $D \geq 3$ there is no longer any multiplication law and there are many different invariants at order n. The colors become essential as a canonical device to keep track of their combinatorics. Colored matrix models can of course still been defined and have been studied in [37].

[6] It is analogous to the universality class of pure $2d$ quantum gravity which is obtained for most values of the coupling constants in one-matrix models [1,8].

to recall that uncolored renormalizable models of this type have been found for rank 3 and rank 4 tensors [59,60]. Again the renormalization in such models is entirely based on a dynamical version of the $1/N$ expansion. One should explore their flows, phase transitions, critical exponents, gauge invariant extensions, and constructive properties, as they seem a promising approach to the quantization of gravity in more than two dimensions [61].

We follow the standard presentation of invariant matrix models in the large N limit, like in the well-known review [1], to emphasize the new status of the field. In Sec. II we define the generic models. In Sec. III we consider their $1/N$ expansion, which is dominated by the melonic graphs and establish their continuum limit. In Sec. IV we analyze the infinite family of multicritical points for these models.

II. THE $1/N$ EXPANSION OF INVARIANT TENSOR MODELS

A. Tensor invariants and action

The models we consider are based on complex tensors which have *no* symmetry between their indices. In order to write the most general action, one must first understand the invariants built from such tensors. It turns out that the analysis of these invariants automatically leads to a representation in colored graphs.

Let $H_1, \ldots, H_D$ be complex vector spaces of dimensions $N_1, \ldots, N_D$. A rank D covariant tensor $T_{n_1 \ldots n_D}$ can be seen as a collection of $\prod_{i=1}^{D} N_i$ complex numbers supplemented with the requirement of covariance under base change. We consider tensors T transforming under the *external* tensor product of fundamental representations of the unitary group $\otimes_{i=1}^{D} U(N_i)$, that is each $U(N_i)$ acts independently on its corresponding H_i. The complex conjugate tensor $\bar{T}_{n_1 \ldots n_D}$ is then a rank D contravariant tensor. They transform as

$$\begin{aligned} T'_{a_1 \ldots a_D} &= \sum_{n_1, \ldots, n_D} U_{a_1 n_1} \ldots V_{a_D n_D} T_{n_1 \ldots n_D}, \\ \bar{T}'_{a_1 \ldots a_D} &= \sum_{n_1, \ldots, n_D} \bar{U}_{a_D n_D} \ldots \bar{V}_{a_1 n_1} \bar{T}_{n_1 \ldots n_D}. \end{aligned} \tag{2.1}$$

From now on we will always denote the indices of the complex conjugated tensor with a bar. We will sometimes denote the D-tuple of integers $(n_1, \ldots, n_D)$ by $\vec{n}$ and assume (unless otherwise specified) $D \geq 3$. We restrict to $H_i = H$, $N_i = N$, for all i.

Among the polynomial quantities one can build out of T and $\bar{T}$ we will deal in the sequel exclusively with *trace invariants*. The trace invariants are built by contracting two by two covariant with contravariant indices in a polynomial in the tensor entries. We write trace invariants formally like

$$\mathrm{Tr}\,(T, \bar{T}) = \sum \prod \delta_{n_1, \bar{n}_1} T_{n_1 \ldots} \ldots \bar{T}_{\bar{n}_1 \ldots}, \tag{2.2}$$

where *all* indices are saturated. Note that a trace invariant has necessarily the same number of T and $\bar{T}$.

Trace invariants can be labeled by graphs with distinguished vertices. To draw the graph associated to a trace invariant we represent every T by a white vertex v and every $\bar{T}$ by a black vertex $\bar{v}$. We promote the position of an index to a color: n_1 has color 1, n_2 has color 2, and so on. The contraction of two indices n_i and $\bar{n}_i$ of tensors is represented by a line $l^i = (v, \bar{v})$ connecting the corresponding two vertices. Lines inherit the color of the index, and always connect a black and a white vertex. Any trace invariant is then represented by a D-colored graph.

Definition 1.—A closed D-colored graph, or *D-bubble*, is a graph $\mathcal{B} = (\mathcal{V}, \mathcal{E})$ with vertex set $\mathcal{V}$ and line set $\mathcal{E}$ such that

(i) $\mathcal{V}$ is bipartite, i.e. there exists a partition of the vertex set $\mathcal{V} = A \cup \bar{A}$, such that for any element $l \in \mathcal{E}$, then $l = \{v, \bar{v}\}$ with $v \in A$ and $\bar{v} \in \bar{A}$. Their cardinalities satisfy $|\mathcal{V}| = 2|A| = 2|\bar{A}|$.

(ii) The line set is partitioned into D subsets $\mathcal{E} = \bigcup_{i=1}^{D} \mathcal{E}^i$, where $\mathcal{E}^i$ is the subset of lines with color i, with $|\mathcal{E}^i| = |A|$.

(iii) It is D-regular (all vertices are D-valent) with all lines incident to a given vertex having distinct colors.

Some examples of trace invariants for rank 3 tensors are represented in Fig. 1. The trace invariant associated to the graph $\mathcal{B}$ writes as

$$\begin{aligned} \mathrm{Tr}_{\mathcal{B}}(T, \bar{T}) &= \sum_{\{\vec{n}^v, \bar{\vec{n}}^{\bar{v}}\}_{v, \bar{v} \in \mathcal{V}}} \delta^{\mathcal{B}}_{\{\vec{n}^v, \bar{\vec{n}}^{\bar{v}}\}} \prod_{v, \bar{v} \in \mathcal{B}} T_{\vec{n}^v} \bar{T}_{\bar{\vec{n}}^{\bar{v}}}, \quad \text{with} \\ \delta^{\mathcal{B}}_{\{\vec{n}^v, \bar{\vec{n}}^{\bar{v}}\}} &= \prod_{i=1}^{D} \prod_{l^i = (v, \bar{v}) \in \mathcal{B}} \delta_{n_i^v \bar{n}_i^{\bar{v}}}, \end{aligned} \tag{2.3}$$

where l^i runs over all the lines of color i of $\mathcal{B}$. We call the $\delta^{\mathcal{B}}_{\{\vec{n}^v, \bar{\vec{n}}^{\bar{v}}\}}$ (the product of delta functions encoding the index contractions of the observable associated to the graph $\mathcal{B}$) the *trace invariant operator with associated graph* $\mathcal{B}$ [42]. Trace invariant operators factor over the connected components of the graph. From now on we will always consider connected invariants, hence invariants associated to connected graphs in the above representation. We denote $\Gamma^{(D)}_{2k}$ the set of D-colored, connected graphs with $2k$ distinguished vertices and $\Gamma^{(D)}$ the set of all graphs with D colors.

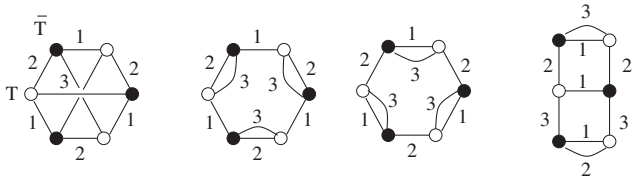

FIG. 1. Graphical representation of trace invariants.

Of particular importance in the sequel are the subgraphs with two colors of a D-colored graph, called *faces*. We denote them $\mathcal{F}$. For instance the graphs with 3 colors posses three type of faces, given by the subgraphs with lines of colors 12, 13, and 23. As every line belongs to exactly two faces (the lines of color 1 belong to a face 12 and a face 13, etc.), the graphs with three colors can be represented as ribbon graphs.

To every graph $\mathcal{B}$ with D colors we can associate a non-negative integer, its *degree* $\omega(\mathcal{B})$ [39,40,43]. We recall its definition and properties in the Appendix. The main feature of the degree is that it provides a counting of the number of faces of a graph, thus for a graph with D colors and $2p$ vertices the total number of faces computes

$$|\mathcal{F}| = \frac{(D-1)(D-2)}{2}p + (D-1) - \frac{2}{(D-2)!}\omega(\mathcal{B}). \quad (2.4)$$

Taking into account that graphs with 3 colors are ribbon graphs, it is easy to see that in this case the degree reduces to the genus. In higher dimensions the degree provides a generalization of the genus. It is *not* a topological invariant, but it combines topological and combinatorial information about the graph.

Going back to invariants one can build out of a complex tensor, we note that there exists a unique D-colored graph with two vertices, namely, the graph in which all the lines connect the two vertices. We call it the D-dipole (denoted $\mathcal{B}_1$) and its associated invariant is

$$\mathrm{Tr}_{\mathcal{B}_1}(T,\bar{T}) = \sum_{\vec{n},\bar{\vec{n}}} T_{\vec{n}}\bar{T}_{\bar{\vec{n}}}\Big[\prod_{i=1}^{D}\delta_{n_i\bar{n}_i}\Big]. \quad (2.5)$$

The most general invariant action for a nonsymmetric tensor is therefore

$$S(T,\bar{T}) = t_1\,\mathrm{Tr}_{\mathcal{B}_1}(T,\bar{T}) + \sum_{k=2}^{\infty}\sum_{\mathcal{B}\in\Gamma_{2k}^{(D)}} t_{\mathcal{B}}N^{-[2/(D-2)!]\omega(\mathcal{B})}\,\mathrm{Tr}_{\mathcal{B}}(T,\bar{T}), \quad (2.6)$$

where $(t_{\mathcal{B}})$ is the set of coupling constants associated to D-bubbles and we singled out the quadratic part corresponding to $\mathcal{B}_1$. In Eq. (2.6) we have added a scaling in N for every trace invariant, proportional to its degree. As the degree is non-negative this scaling is a suppression of some invariants. We have included it because it simplifies some equations in the following, but we emphasize that this scaling is *not* required. As the reader can check, all the results we present below can be obtained (albeit with some effort) also in its absence. Because of symmetry under relabeling of the black and white vertices, some couplings in (2.6) are redundant. It is however more convenient to assign a distinct coupling constant to each graph with labeled vertices, and remember this redundancy only at the end.

We will deal in this paper with the most general single-tensor model of rank D defined by the partition function

$$Z(t_{\mathcal{B}}) = \exp(-F(t_{\mathcal{B}})) = \int d\bar{T}dT\exp(-N^{D-1}S(T,\bar{T})). \quad (2.7)$$

B. Graph amplitudes

The invariant observables are the trace invariants represented by D-colored graphs. The Feynman graphs contributing to the expectation of an observable are obtained by Taylor expanding with respect to $t_{\mathcal{B}}$ and evaluating the Gaussian integral in terms of Wick contractions. A moment of reflection reveals that the Feynman graphs are made of *effective vertices* $\mathrm{Tr}_{\mathcal{B}}(T,\bar{T})$ (that is graphs $\mathcal{B}$ with colors $1,\ldots,D$) connected by effective *propagators* (Wick contractions, pairings of T's and $\bar{T}$'s). A Wick contraction of two tensor entries $T_{a_1\ldots a_D}$ and $\bar{T}_{\bar{p}_1\ldots\bar{p}_D}$ with the quadratic part (2.5) consists in replacing them by $(1/[N^{D-1}t_1])\times\prod_{i=1}^{D}\delta_{a_i\bar{p}_i}$. The Wick contractions will be represented as dashed lines labeled by the fictitious color 0. Thus every dashed line of color 0 in a Feynman graph identifies *all* the indices of the two vertices (one white corresponding to T and one black corresponding to $\bar{T}$) it connects. An example of a Feynman graph is presented in Fig. 2.

The Feynman graphs are therefore $(D+1)$-colored graphs $\mathcal{G}$. We reserve the notation $\mathcal{B}$ for the D-colored graphs, and $\mathcal{G}$ for the $(D+1)$-colored graphs. A graph $\mathcal{G}$ has two kinds of faces: those with colors $i,j=1,\ldots,D$, denoted $\mathcal{F}_{ij}$ (which belong also to some D-bubble $\mathcal{B}$) and those with colors $0,i$, for $i=1,\ldots,D$, denoted $\mathcal{F}_{0i}$, which involve the lines of color 0 in $\mathcal{G}$.

The free energy has an expansion in closed, connected $(D+1)$-colored graphs,

$$F(t_{\mathcal{B}}) = \sum_{\mathcal{G}\in\Gamma^{(D+1)}}\frac{(-1)^{|\rho|}}{s(\mathcal{G})}A(\mathcal{G}), \quad (2.8)$$

where $s(\mathcal{G})$ is a symmetry factor and $|\rho|$ is the number of effective vertices, i.e. D-bubbles (subgraphs with colors

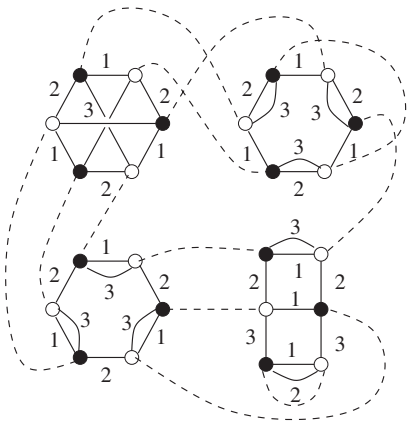

FIG. 2. A Feynman graph.

$1, \ldots, D$). We denote these D-bubbles $\mathcal{B}_{(\rho)}$, with $\rho = 1, \ldots, |\rho|$. The amplitude of a graph is

$$A(\mathcal{G}) = \prod_{\rho} t_{\mathcal{B}_{(\rho)}} \sum_{\{\vec{n}^v, \bar{\vec{n}}^{\bar{v}}\}} \left[\prod_{\rho} N^{D-1-[2/(D-2)!]\omega(\mathcal{B}_{(\rho)})} \delta^{\mathcal{B}_{(\rho)}}_{\{\vec{n}^v, \bar{\vec{n}}^{\bar{v}}\}} \right] \times \left[\prod_{l^0=(v,\bar{v})\in\mathcal{E}^0} \frac{1}{t_1 N^{D-1}} \prod_i \delta_{n_i^v, \bar{n}_i^{\bar{v}}} \right]. \tag{2.9}$$

An index n_i is identified along the lines of color i in $\mathcal{B}_{(\rho)}$ and along the dashed lines of color 0. We thus obtain a free sum per face of colors $0i$, so that

$$A(\mathcal{G}) = \frac{\prod_\rho t_{\mathcal{B}_{(\rho)}}}{t_1^{|l^0|}} N^{(D-1)|\rho| - [2/(D-2)!]\sum_\rho \omega(\mathcal{B}_{(\rho)}) - (D-1)|l^0| + \sum_i |\mathcal{F}_{0i}|}. \tag{2.10}$$

Noting that $\sum_i |\mathcal{F}_{0i}| = |\mathcal{F}| - \sum_\rho |\mathcal{F}_{(\rho)}|$, where $|\mathcal{F}|$ denotes the total number of faces of $\mathcal{G}$ and $|\mathcal{F}_{(\rho)}|$ the number of faces of the D-bubble $\mathcal{B}_{(\rho)}$, using (2.4) for each $\mathcal{B}_{(\rho)}$ and for $\mathcal{G}$ (taking into account that $\mathcal{G}$ has $D+1$ colors) and noting that $|l^0| = p$, with p the half-number of vertices of $\mathcal{G}$, the amplitude of $\mathcal{G}$ computes

$$A(\mathcal{G}) = \frac{\prod_\rho t_{\mathcal{B}_{(\rho)}}}{t_1^p} N^{D-[2/(D-1)!]\omega(\mathcal{G})}, \tag{2.11}$$

with $\omega(\mathcal{G})$ the degree of the graph $\mathcal{G}$. The $1/N$ expansion of the free energy writes

$$F(t_{\mathcal{B}}) = N^D \sum_{\mathcal{G}\in\Gamma^{(D+1)}} \frac{(-1)^{|\rho|}}{s(\mathcal{G})} \frac{\prod_\rho t_{\mathcal{B}_{(\rho)}}}{t_1^p} N^{-[2/(D-1)!]\omega(\mathcal{G})}. \tag{2.12}$$

The leading scaling with N of the free energy is $F(t_{\mathcal{B}}) \sim N^D$. In the rest of this paper we focus on the leading order free energy $f_0(t_{\mathcal{B}}) = \lim_{N\to\infty} N^{-D} F(t_{\mathcal{B}})$. Expectation values of bubble observables have similar expansions. If $\mathcal{B}$ is a D-colored graph, the connected expectation value

$$\frac{1}{N} \frac{\langle \mathrm{Tr}_{\mathcal{B}}(T, \bar{T})\rangle}{Z} = \frac{1}{N^D} N^{[2/(D-2)!]\omega(\mathcal{B})} \frac{\partial F}{\partial t_{\mathcal{B}}} = \sum_{\mathcal{G}\in\Gamma^{(D+1)}, \mathcal{G}\supset\mathcal{B}} \frac{(-1)^{|\rho|}}{s(\mathcal{G})} \times \frac{\prod_\rho t_{\mathcal{B}_{(\rho)}}}{t_1^p} N^{-[2/(D-1)!]\omega(\mathcal{G}) + [2/(D-2)!]\omega(\mathcal{B})}, \tag{2.13}$$

has an expansion in connected $(D+1)$-colored vacuum graphs $\mathcal{G}$ having $\mathcal{B}$ as a (marked) subgraph, denoted $\mathcal{G} \supset \mathcal{B}$. The scaling in N in (2.13) of a graph $\mathcal{G}$ rewrites

$$N^{-(2/D!)\omega(\mathcal{G})} N^{-[2/D(D-2)!](\omega(\mathcal{G}) - D\omega(\mathcal{B}))}. \tag{2.14}$$

Using (a weaker version of) Proposition 2 in the Appendix, $\omega(\mathcal{G}) \geq D\omega(\mathcal{B})$ and the inequality is saturated for $\omega(\mathcal{G}) = 0$. It follows that in the large N limit only graphs $\mathcal{G} \supset \mathcal{B}$ of degree zero contribute to the expectation.

C. Topology from bubbles

To simplify the discussion, in this section we will restrict to the case $D = 3$. The original idea of tensor models [28–30] was to generate triangulations of three-dimensional spaces. The basic building block in the original proposals was an interaction term which combinatorially describes a tetrahedron (a 3-simplex) also used in group field theories [58]

$$V_{\text{tetrahedron}} = \sum_{a,b,c,d,e,f} T_{abc} T_{cde} T_{ebf} T_{fda}. \tag{2.15}$$

This term is not $\otimes^3 U(N)$ invariant. The most one can say about it is that it is invariant under a simultaneous $O(N)$ orthogonal transformation of all its indices.

The situation is already improved in colored tensor models [34] where the indices are distinguished and one can implement a $\otimes^3 U(N)$ invariance. As the pattern of contraction of a tetrahedron is not a trace invariant one can raise the question of the topological interpretation of the trace invariant observables and their relation to triangulations.

The situation is actually like in one-matrix models with generic interactions. A $\mathrm{Tr}(M^k)$-vertex is seen (by duality) as a polygon with k sides. A closed graph is then a gluing of such polygons. Obviously one can divide each polygon into triangles (by adding a vertex in the middle of the polygon, i.e. by taking the topological cone over its boundary), so that the graph encodes a triangulation. Here, a similar interpretation holds. The $(3+1)$-colored graphs are known to describe topological 3-dimensional pseudo-manifolds [34]. The black and white vertices of the graph correspond to tetrahedra (3-simplices). The triangles (2-simplices) bounding a tetrahedron are represented by the half-lines touching the vertex, hence are colored 0, 1, 2, 3. The lower dimensional simplices are colored by the colors of the triangles sharing them. Thus the edges are labeled by pairs of colors (the edge 12 is common to the triangles 1 and 2), and the points (vertices of the tetrahedra, to be distinguished from the vertices of the graph) are labeled by triples of colors (the point 123 is the point common to the triangles 1, 2 and 3 bounding a tetrahedron).

A line in the colored graph represents the unique gluing of two tetrahedra of opposite orientations along boundary triangles which respects *all* the colorings; that is we glue triangles of the same color, say 2, in such a way that the edge 02 (respectively 12 and 32) bounding a triangle is glued on the edge 02 (respectively 12 and 32) bounding the second triangle, and similarly for points. This construction yields the pseudomanifold dual to a $(3+1)$-colored graph.

Alternatively the same graph with $3+1$ colors can be seen as the gluing of the effective interactions, $\mathcal{B}$ which are

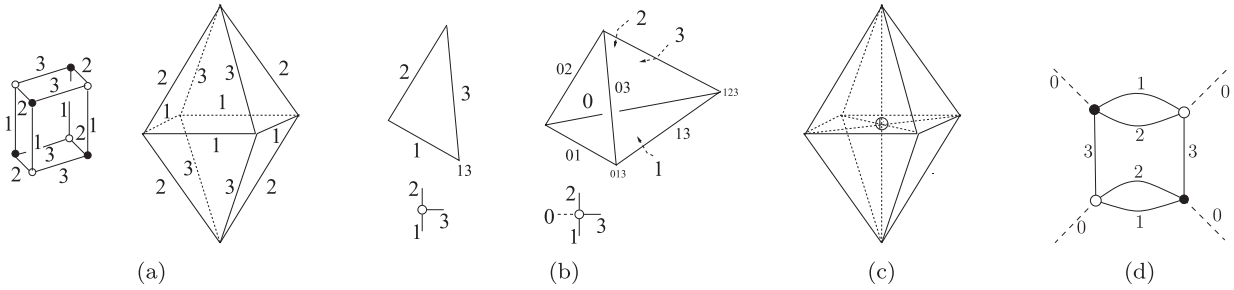

FIG. 3. Trace invariants and gluings of simplices in $D = 3$.

graphs with 3 colors, along the lines of color 0. Following the above construction, each effective interaction by itself, being a graph with 3 colors, represents a surface. The (black and white) vertices are dual to triangles, and the edges bounding the triangles are colored 1, 2 and 3. The surface represented by an interaction is the unique one obtained by gluing the triangles along their edges (as indicated by the graph with three colors) respecting all the colorings (i.e. those of the edges and of the points). In Fig. 3(a) for instance we represented such a surface obtained by gluing eight triangles.

Adding the lines of color 0 results in taking the topological cone over this pseudomanifold, $C_M = (M \times [0, 1])/(M \times \{1\})$. Let us first examine the effect of this coning on one triangle [represented in Fig. 3(b)]. The original triangle will now be called a triangle of color 0 [see Fig. 3(b)]. The original edges acquire the new color 0, hence they will be called 01, 02 and 03 [see again Fig. 3(b)], and similarly the original points (13 becomes 013, etc.). This coning adds extra triangles, edges, and points. Every original edge gives by coning a new triangle. We color this triangle by the color of the edge, hence the original edge of color 1 gives rise by coning to the triangle of color 1 [see again Fig. 3(b)]. Note that the new triangle 1 shares with the original triangle, 0 the edge 01. Every original point gives by coning an edge, which inherits the colors of the original point (the edge 13 is the cone over the original point 13 and is shared by the triangles 1 and 3). We also obtain a new point labeled 123. When taking the cone over the surface defined by a connected graph $\mathcal{B}$ (with colors 1, 2 and 3), we obtain new triangles (one for every edge of the surface), new edges (one for every point of the surface), and an unique new point 123, the apex of the cone.

Thus, when seen as a subgraph of a $(3 + 1)$-colored graph $\mathcal{G}$, $\mathcal{B}$ represents a ''chunk'' of the three-dimensional space. For the example of the graph with 3 colors in Fig. 3 (a) adding the dashed lines of color 0, we obtain the gluing of 8 tetrahedra drawn in Fig. 3(c). This chunk has the topology of a ball and is bounded by the 8 triangles of color 0 corresponding to the dashed half-lines.

Thus the trace invariant quartic interactions like

$$\sum_{n_i,m_i} T_{n_1n_2n_3}\bar{T}_{n_1n_2m_3}T_{m_1m_2m_3}\bar{T}_{m_1m_2n_3}, \qquad (2.16)$$

represented in Fig. 3(d), correspond to a gluing of four tetrahedra, with four external, boundary triangles of color 0, and not to a tetrahedron. Note that a chunk can have a nontrivial topology, for instance it can be a cone over a torus.

One can employ an alternative *stranded graph* representation of the Feynman graphs, closer to the ribbon graph representation of matrix models. This is presented in Fig. 4(a). One replaces the black and white vertices of the effective interactions by stranded halflines, which are then connected by dashed lines having each three strands. In this representation the strands colored 1, 2, and 3 have each an associated Kronecker δ which corresponds to the contraction of a tensor index between two tensors of the bubble observable. The dashed lines have three strands representing the three Kronecker δ coming from a Wick contraction which propagate the tensor indices. The faces of colors $0i$ are easily identifiable. Each stranded halfline corresponds to a triangle (the triangles of color 0 in the colored graph representation). The graph of the effective interaction encodes the pattern of gluing of the triangles into a surface (the boundary of a chunk), and the dashed lines encode the gluing of chunks along boundary triangles. As this representation is redundant and somewhat cumbersome we will not use it further.

Before concluding this section let us remark that the fact that the graphs are bipartite plays a secondary role, ensuring just the orientability [62]. What is crucial is that a colored graph represents the unique gluing of simplices which respects *all* the labelling (including the induced ones over all the lower dimensional simplices). Dropping the bipartite requirement allows one to consider the $O(N)^3$ invariant presented in Fig. 4(b). As it consists in a gluing of four triangles and any two triangles share exactly one edge one might be tempted to interpret it as a gluing pattern

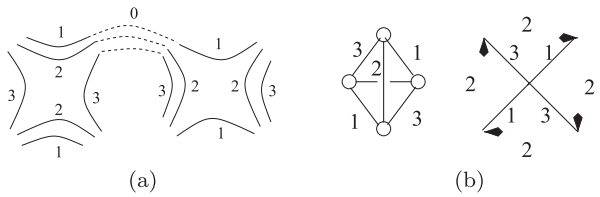

FIG. 4. Stranded graph and a nonbipartite invariant.

of four triangles bounding a tetrahedron. However, this interpretation is not the correct one. Indeed, on closer inspection, it turns out that the dual gluing consists in four triangles glued first around a vertex (say 13) and then glued along opposite edges of color 2 [see the right hand side of Fig. 4(b)]. Thus, respecting the rules of the colored gluings described above, this $O(N)^3$ invariant has the topology of the real projective plane $\mathbb{R}P^2$.

III. LARGE N LIMIT

A. The melonic family and the large N factorization

In the large N limit, only graphs with vanishing degree survive. For $(2+1)$-colored graphs the degree is the genus of the graph, hence the graphs of degree 0 are exactly the planar graphs and represent spheres. For $D \geq 3$, the $(D+1)$-colored graphs $\mathcal{G}$ with $\omega(\mathcal{G}) = 0$ have been shown to also describe topological spheres in dimension D [40,41,43].

1. Combinatorial description of melons

We explain in the Appendix why the $(D+1)$-colored graphs of degree zero, called *melonic*, can be obtained by the insertion procedure detailed below. While the dominant graphs of our models are melonic, it is understood that not all melonic graphs are generated. However, this section is only concerned with the combinatorial properties of the melonic family, hence we temporarily allow ourselves to also use melonic graphs which do not appear in the Feynman expansion of our models.

First order.—The lowest order graph consists in two vertices connected by $(D+1)$ lines, as in the Fig. 5(a). We consider all lines incident at the positive (black) vertex to be *active*, which means that higher order graphs will be obtained by insertions on them.

Second order.—$(D+1)$ graphs contribute to the second order. They arise from inserting two vertices connected by D lines on any of the $(D+1)$ active lines of the first order graph. If the line on which we insert this decoration has color i, the new lines will be colored by all colors except i. Let us say we insert this graph on the active line of color 1, like in the Fig. 5(b) (hence the new lines have colors 2, 3 up to D). All lines incident at the new black vertex are deemed active (the new lines of colors $2, \ldots, D$ as well as the external line of color 1), while the exterior line of color 1 incident at the new white vertex [in bold in Fig. 5(b)] is deemed inactive.

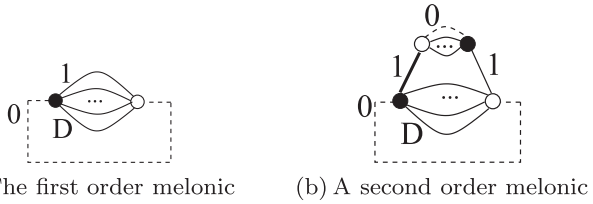

(a) The first order melonic graph. (b) A second order melonic graph.

FIG. 5. Melonic graphs at first and second orders.

Order $p+1$.—We obtain the graphs at order $p+1$ by inserting two vertices connected by D lines (with appropriate colors) on any of the active lines of a graph at order p. Once again, with respect to the new vertices, all lines incident to the black vertex are deemed active, while the exterior line incident to its white vertex is deemed inactive.

We are now going to show that the expectation values of melonic graphs are fully determined by the (dressed) covariance of the model, in a specific, factorized form.

2. Large N factorization

In the large N limit, only the bubble observables $\mathcal{B}$ for which there exist $D+1$-colored graphs $\mathcal{G}$ which are melonic survive. The melonic graphs have some important properties, which put together lead to the large N factorization of expectations.

(i) If a $(D+1)$-colored graph $\mathcal{G}$ is melonic then all its subgraphs $\mathcal{B}$ with colors $1, 2, \ldots, D$ are melonic see Fig. 6(a) and are therefore built following the same procedure.

(ii) In this procedure, $\mathcal{G}$ is obtained by inserting pairs of vertices v and $\bar{v}$ separated by D lines, and a D-colored subgraph $\mathcal{B}$ is obtained by performing the same insertions, but ignoring the color 0.

(iii) Consider two vertices v and $\bar{v}$ inserted at some step. At the time of the insertion, they are connected in $\mathcal{G}$ by D lines and some two-point graph (corresponding to the line on which they have been inserted). As all further insertions are made on the lines of $\mathcal{G}$, the two half-lines of any color (0, 1, up to D) on v and $\bar{v}$ will always be connected together via two-point graphs.

Therefore, for every such pair of vertices v and $\bar{v}$ of $\mathcal{B}$, the two half-lines of color 0 must be connected via some two-point graph in $\mathcal{G}$ [see Fig. 6(b)]. In other words, starting with a melonic D-colored observable, there is a *unique* way to pair its external halflines with two-point insertions so as to get melonic $(D+1)$-colored graphs. Then, the full expectation value is obtained by inserting this way full two-point functions, one for each pair of vertices which are joined.

As a result, in the $N \to \infty$ limit, the expectation of a melonic observable factors in terms of full two-point functions (dressed propagators). The full two-point function writes

$$\frac{1}{Z}\langle T_{n_1 \ldots n_D} T_{\bar{n}_1 \ldots \bar{n}_D} \rangle = \frac{\prod_{i=1}^{D} \delta_{n_i, \bar{n}_i}}{N^{D-1}} U(t_{\mathcal{B}}, N), \qquad U(t_{\mathcal{B}}, N) = \frac{1}{t_1} + \ldots, \tag{3.1}$$

where $(1/t_1)$ is the bare propagator and the dots denote the radiative corrections. We denote $\lim_{N\to\infty} U(t_{\mathcal{B}}, N) =$

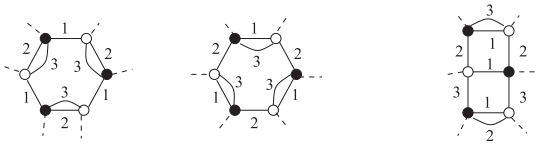

(a) Melonic observables.

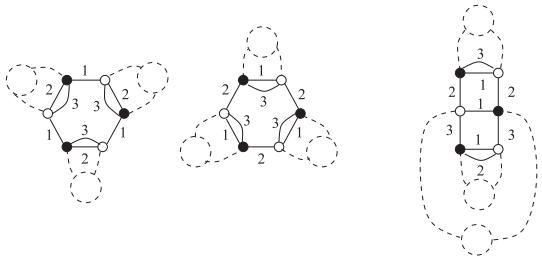

(b) Graphs contributing to the melonic observables.

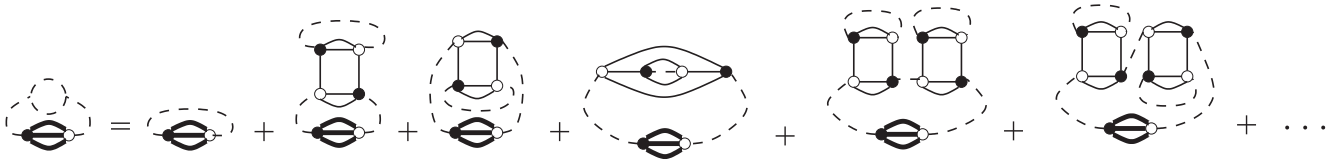

FIG. 6. Graphs contributing to the 3-dipole expectation.

$U(t_{\mathcal{B}})$. The large N expectation of the D-dipole observable $\mathcal{B}_1$ computes then

$$\lim_{N\to\infty}\frac{1}{N}\frac{\langle \mathrm{Tr}_{\mathcal{B}_1}(T,\bar{T})\rangle}{Z}=U(t_{\mathcal{B}}). \tag{3.2}$$

Some graphs contributing to this expectation for $D=3$ are presented in Fig. 6, where the marked graph $\mathcal{B}_1$ is presented in bold. The colors of the lines are assigned turning clockwise 0, 1, 2, and 3 at the white vertices.

We thus conclude that

$$\lim_{N\to\infty}\frac{1}{N}\frac{\langle \mathrm{Tr}_{\mathcal{B}}(T,\bar{T})\rangle}{Z} = \begin{cases} 0 & \text{if } \mathcal{B} \text{ is not melonic} \\ U(t_{\mathcal{B}})^{p_{\mathcal{B}}}, & \text{if } \mathcal{B} \text{ is melonic with } 2p_{\mathcal{B}} \text{ vertices} \end{cases}. \tag{3.3}$$

In particular this factorization holds for the Gaussian model with $t_{\mathcal{B}}=0$ for $\mathcal{B}\neq\mathcal{B}_1$, and the full two-point function simply given by the bare covariance $U(t_{\mathcal{B}})=1/t_1$.

The universality of tensor measures, first derived in [56] (where it was obtained by mapping melons to trees), is the fact that the observables satisfy (3.3). It means that in the large N limit the models become Gaussian. However this large N limit is very nontrivial, as the covariance of the large N Gaussian is the *full*, resummed, two-point function. The rest of this paper is dedicated to explore the various multicritical behaviors and continuum limits governed by this resummed covariance.

B. The leading order two-point function and free energy

The full two-point function at large N is determined by a self-consistency equation provided by a Schwinger-Dyson equation supplemented with the above factorization. The relevant Schwinger-Dyson equation is

$$\frac{1}{N^D}\sum_{n_1\ldots,n_D}\frac{1}{Z}\int dT d\bar{T}\frac{\partial}{\partial T_{n_1\ldots n_D}}[T_{n_1\ldots n_D}e^{-N^{D-1}S(T,\bar{T})}]=0. \tag{3.4}$$

Taking the derivative explicitly, one gets

$$1-\sum_{\mathcal{B}}p_{\mathcal{B}}t_{\mathcal{B}}\frac{1}{N}\frac{\langle \mathrm{Tr}_{\mathcal{B}}(T,\bar{T})\rangle}{Z}=0, \tag{3.5}$$

where $p_{\mathcal{B}}$ denotes the half-number of vertices of the bubble $\mathcal{B}$ (that is the number of either black or white vertices). At leading order in $1/N$ this can be rewritten in the following form. We first define the leading order potential

$$\begin{aligned} V(x,t_{\mathcal{B}}) &= \sum_{n\geq 1}\Big(\sum_{\substack{\mathcal{B}\ \text{melonic},\\ p_{\mathcal{B}}=n}} t_{\mathcal{B}}\Big)x^n, \\ V'(x,t_{\mathcal{B}}) &\equiv \frac{\partial V}{\partial x}(x,t_{\mathcal{B}}) = \sum_{n\geq 1} n\Big(\sum_{\substack{\mathcal{B}\ \text{melonic},\\ p_{\mathcal{B}}=n}} t_{\mathcal{B}}\Big)x^{n-1}, \end{aligned} \tag{3.6}$$

and taking into account the factorization of the melonic expectations, the Schwinger-Dyson equation becomes the following self-consistency equation

$$U(t_{\mathcal{B}})V'(U(t_{\mathcal{B}}),t_{\mathcal{B}})=1. \tag{3.7}$$

The leading order two-point function is the solution of this polynomial equation whose coefficients are the coupling constants of melonic observables.

Once U is determined using (3.7), one can access the free energy f_0. The leading order free energy $f_0(t_{\mathcal{B}})$, like the leading order potential $V(x,t_{\mathcal{B}})=\sum_{n\geq 1}(\sum_{\substack{\mathcal{B}\ \text{melonic},\\ p_{\mathcal{B}}=n}} t_{\mathcal{B}})x^n$ and the leading order two-point function $U(t_{\mathcal{B}})$ only depends on the coupling constants of the melonic bubbles $t_{\mathcal{B}}$. Consider the function $f_0 - V(U(t_{\mathcal{B}}),t_{\mathcal{B}})+\ln U(t_{\mathcal{B}})$. Its differential is

$$d[f_0 - V(U(t_{\mathcal{B}}), t_{\mathcal{B}}) + \ln U(t_{\mathcal{B}})] = \sum_{\mathcal{B}\ \text{melonic}} \left[\frac{\partial f_0}{\partial t_{\mathcal{B}}} - U(t_{\mathcal{B}})^{p_{\mathcal{B}}} - V'(U(t_{\mathcal{B}}), t_{\mathcal{B}})\frac{\partial U}{\partial t_{\mathcal{B}}} + \frac{1}{U(t_{\mathcal{B}})}\frac{\partial U}{\partial t_{\mathcal{B}}}\right] dt_{\mathcal{B}} = 0. \tag{3.8}$$

Thus the leading order free energy is

$$f_0(t_{\mathcal{B}}) = V(U(t_{\mathcal{B}}), t_{\mathcal{B}}) - \ln U(t_{\mathcal{B}}). \tag{3.9}$$

C. The continuum limit

Tensor models are of combinatorial nature and as such provide a notion of continuum limit in a combinatorial way. The idea is that disregarding the geometrical content and interpretation which may be given to a model, this limit is always obtained as the regime where graphs with a very large number of vertices dominate. As an illustration, we derive the continuum limit in a particular T^4 truncation defined by the action

$$S_{T^4}(T, \bar{T}) = \sum_{\vec{n}} T_{\vec{n}} \bar{T}_{\vec{n}} + g \sum_{\substack{a_1,\ldots,a_D \\ b_1,\ldots,b_D}} T_{a_1\ldots a_{D-1}a_D} \bar{T}_{a_1\ldots a_{D-1}b_D} T_{b_1\ldots b_{D-1}b_D} \bar{T}_{b_1\ldots b_{D-1}a_D}. \tag{3.10}$$

Note that the interaction term is melonic. The leading order potential is defined by $t_1 = 1$, $t_2 = g$, that is $V(x) = x + gx^2$. The leading order free energy is therefore

$$f_0(g) = \sum_{n\in\mathbb{N}} g^n f^{(4n)}, \tag{3.11}$$

where $f^{(4n)}$ is the number of $(D+1)$-colored melonic graphs built with n effective interactions T^4 (thus having $4n$ black and white vertices). The number $f^{(4n)}$ is a canonical partition function for graphs with fixed number of vertices and $f_0(g)$ is its associated grand-canonical partition function with lattice "chemical potential" g. The thermodynamic limit is encoded into the asymptotic behavior of $f^{(4n)}$,

$$f^{(4n)} \sim_{n\to\infty} A n^{\gamma-3} g_c^{-n}, \tag{3.12}$$

for some constants A, g_c and γ. Thus g_c is the radius of convergence of $f_0(g)$, which means that when g approaches g_c, $f_0(g)$ loses its summability and graphs with a large number of vertices $(4n)$ dominate its behavior. The power-law decay characterized by γ controls the singularity of $f_0(g)$ close to g_c, since

$$f_0(g) \sim |g - g_c|^{2-\gamma}. \tag{3.13}$$

The exponent γ is known as the entropy exponent.[7] Let us compute the entropy exponent of the model defined by S_{T^4}. First one notices that the derivative of the leading order free energy writes in terms of the leading order two-point function $\frac{\partial f_0}{\partial g} = U(g)^2$. The Eq. (3.7) gives

$$2gU(g)^2 + U(g) - 1 = 0, \quad \text{hence } U(g) = \frac{\sqrt{1+8g} - 1}{4g}, \tag{3.14}$$

where we selected the physical root with initial condition $U(0) = 1$. One thus identifies $g_c = -1/8$ and for $g \to g_c$ the nonanalytic parts of the two-point function and free energy are

$$U(g)_{\text{sing}} \sim (g - g_c)^{1/2}, \quad f_{0,\text{sing}} \sim (g - g_c)^{3/2}, \quad \text{hence } \gamma = 1/2. \tag{3.15}$$

The average number of effective interactions (proportional to the number of vertices) diverges when tuning to criticality

$$\langle n \rangle = g\frac{\partial}{\partial g}\log f_0 \sim \frac{1}{|g - g_c|} \underset{g\to g_c}{\to} \infty. \tag{3.16}$$

D. Virasoro constraints

We now come back to the generic model with arbitrary couplings. The full set of Schwinger-Dyson equations is obtained by inserting generic D-bubble observables in (3.4). The equations can be recast as $L_{\mathcal{B}} Z(t_{\mathcal{B}}) = 0$ for some differential operators $L_{\mathcal{B}}$ labeled by the observables. The algebra of these operators has been discussed at length in [56]. Because of the large N factorization one can find the leading order Schwinger-Dyson equations and the associated algebra of constraints by a shorter route. We show below that the large N factorization (3.3) reduces the Schwinger-Dyson equations to a set of Virasoro constraints, like in matrix models. We emphasize that this only holds at leading order in $1/N$.

Note that in fact the leading order two-point function $U(t_{\mathcal{B}})$ as well as the leading order free energy f_0 depend only on the sums of the coupling constants of melonic observables at fixed number of vertices. Thus, defining $t_n \equiv \sum_{\mathcal{B}\ \text{melonic}, p_{\mathcal{B}}=n} t_{\mathcal{B}}$, the large N factorization becomes

[7] In the $\mathrm{Tr}\, M^4$ matrix model for random two-dimensional lattices for instance one has $\gamma = -1/2$ [1], which is the universality class of pure two-dimensional quantum gravity. As such, it is reached generically, i.e. for most values of the coupling constants, in the continuum limit of one-matrix models.

$$\frac{\partial f_0}{\partial t_n} = [U(t_p)]^n, \tag{3.17}$$

Then multiplying (3.7) by U^k for any positive k we get

$$[U(t_p)]^k - \sum_{n\geq 1} n t_n [U(t_p)]^{n+k} = 0, \quad \forall\ k \geq 0. \tag{3.18}$$

These equations can be seen as differential equations on f_0,

$$L_k f_0 = 0, \quad \text{for} \quad L_k = \frac{\partial}{\partial t_k} - \sum_{n\geq 1} n t_n \frac{\partial}{\partial t_{n+k}}. \tag{3.19}$$

It is straightforward to check that the differential operators satisfy the well-known algebra

$$[L_n, L_m] = (m-n) L_{m+n}. \tag{3.20}$$

IV. MULTICRITICAL BEHAVIORS IN THE LARGE N LIMIT

We now set the summed coupling constants $t_1 = 1/g$, and $t_n = \alpha_n/g$ to investigate the different possible critical behaviors with respect to the parameter g. The potential V becomes $V(x) = (x + \sum_{k=2} \alpha_k x^k)/g$. The self-consistency Eq. (3.7) for the two-point function becomes

$$g = U + \sum_{k=2}^{m} k \alpha_k U^k. \tag{4.1}$$

Like in the matrix models review [1], the continuum limit is obtained by setting $\partial g/\partial U = 0$. At least locally, this equation can be solved for U in terms of the parameters α_k. One concludes that for generic values of these parameters $\gamma = 1/2$, thus proving the universality of this continuum limit, first derived in [41] for the colored model.

However, there are points on the set of parameters where the equation $\partial g/\partial U = 0$ can not be solved for U, because $\partial^2 g/\partial U^2$ may vanish and there the implicit function theorem can not be applied. In these cases, one has multicritical behaviors and $\gamma > 1/2$. A multicritical point of order m is defined, like in one-matrix models, by

$$\frac{\partial g}{\partial U} = \cdots = \frac{\partial^{m-1} g}{\partial U^{m-1}} = 0, \quad \text{and} \quad \frac{\partial^m g}{\partial U^m} \neq 0, \tag{4.2}$$

which imply $g = g_c - (U_c - U)^m + \mathcal{O}((U - U_c)^{m+1})$. Such multicritical behaviors have already been observed in tensor models in [48] (where they are interpreted in terms of dimer models) and [53]. As g is a polynomial in U whose coefficients α_k can be freely chosen, multicritical points can be reached for the generic one-tensor model. We present below a minimal realization, i.e. a potential V with minimal degree leading to a multicritical point of order m. We first set $U_c = m^{-1/(m-1)}$, and consider

$$V(U) = \frac{1}{g} \sum_{k=1}^{m} \frac{1}{k} U_c^{m-k} [U_c^k - (U_c - U)^k]. \tag{4.3}$$

Thus V is of degree m, satisfies $V(0) = 0$, the coefficient of the linear term is $1/g$ and $UV'(U) = [U_c^m - (U_c - U)^m]/g$. The self-consistency equation is exactly

$$g = g_c - (U_c - U)^m, \quad \text{with} \quad g_c = U_c^m. \tag{4.4}$$

Substituting into (3.9) we find

$$\begin{aligned} f_0 &= \frac{1}{g} \sum_{k=1}^{m} \frac{1}{k} U_c^{m-k} [U_c^k - (U_c - U)^k] - \ln[U_c - (U_c - U)] \\ &= f_0(g_c) - \frac{U_c^m}{g} \sum_{k=1}^{m} \frac{1}{k} \left(\frac{U_c - U}{U_c}\right)^k + \sum_{k=1}^{\infty} \frac{1}{k} \left(\frac{U_c - U}{U_c}\right)^k \\ &\quad + \left[\frac{1}{g} - \frac{1}{g_c}\right] \sum_{k=1}^{m} \frac{1}{k} U_c^m. \end{aligned} \tag{4.5}$$

Taking into account that $U_c - U = (g_c - g)^{1/m}$, we obtain for $g \to g_c$

$$\begin{aligned} f_0 &= f_0(g_c) + \left(\sum_{k=1}^{m} \frac{1}{k}\right)\left(\frac{g_c - g}{g_c}\right) - \frac{m}{(m+1)} \\ &\quad \times \left(\frac{g_c - g}{g_c}\right)^{1+(1/m)} + \mathcal{O}((g_c - g)^{1+(2/m)}), \end{aligned} \tag{4.6}$$

hence a multicritical entropy exponent $\gamma_m = 1 - 1/m$, as obtained in [53] and in [48], coinciding with the ones of multicritical branched polymers [55].

ACKNOWLEDGMENTS

Research at Perimeter Institute is supported by the Government of Canada through Industry Canada and by the Province of Ontario through the Ministry of Research and Innovation.

APPENDIX: COMBINATORICS OF COLORED GRAPHS: JACKETS, DEGREE AND MELONS

In order to define the degree of a graph one first needs the notion of *jacket* [38–40].

Definition 2.—Let $\mathcal{B}$ be a D-colored graph and τ be a cycle on $\{1, \ldots, D\}$. A colored *jacket* $\mathcal{J}$ of $\mathcal{B}$ is a ribbon graph having all the vertices and all the lines of $\mathcal{B}$, but only the faces with colors $(\tau^q(1), \tau^{q+1}(1))$, for $q = 0, \ldots, D-1$, modulo the orientation of the cycle.

As a jacket $\mathcal{J}$ of $\mathcal{B}$ contains all the vertices and all the lines of $\mathcal{B}$, $\mathcal{J}$ and $\mathcal{B}$ have the same connectivity. As such, any jacket $\mathcal{J}$ carries some key topological information about $\mathcal{B}$ (for instance the fundamental group of $\mathcal{B}$ is a subgroup of the fundamental group of any of its jackets [47]). For graphs with four colors, the jackets correspond to Heegaard splitting surfaces [49].

Jackets are ribbon graphs, hence they are completely classified by their genus $g_{\mathcal{J}}$.

Definition 3.—The *degree* $\omega(\mathcal{B})$ of a colored graph $\mathcal{B}$ is the sum of genera of its jackets, $\omega(\mathcal{B}) = \sum_{\mathcal{J}} g_{\mathcal{J}}$.

Graphs with three colors are ribbon graphs, and the degree coincides with the genus. The crucial property of the degree is that the total number of faces $\mathcal{F}$ of a D-colored graph computes in terms of the degree.

Proposition 1.—Let $\mathcal{B}$ a D-colored graph with $2p$ vertices. Then the total number of faces of $\mathcal{B}$ respects

$$|\mathcal{F}| = \frac{(D-1)(D-2)}{2}p + (D-1) - \frac{2}{(D-2)!}\omega(\mathcal{B}). \tag{A1}$$

Proof.—This equation can be found in the literature (see [40] for instance). However, due to its importance we present here its proof. Every jacket is a ribbon graph with $2p$ vertices and Dp lines, hence the number of faces of a jacket is

$$|\mathcal{F}_{\mathcal{J}}| = (D-2)p + 2 - 2g_{\mathcal{J}}. \tag{A2}$$

As jackets correspond to cycles over D elements modulo the orientation, $\mathcal{B}$ has $\frac{1}{2}(D-1)!$ distinct jackets. The faces with colors ij will belong to the $2(D-2)!$ jackets corresponding to the cycles π such that $\pi(i) = j$ and $\pi(j) = i$. Moding by the orientation we conclude that each face belongs to exactly $(D-2)!$ distinct jackets. Summing (A2) over the jackets and dividing by $\frac{1}{2}(D-1)!$ proves the lemma.

Of course the same definition goes trough for graphs $\mathcal{G}$ with $D+1$ colors. Further facts concerning the degree are listed below.

Proposition 2.—The degrees of a $(D+1)$-colored graph $\mathcal{G}$ and of its D-bubbles $\mathcal{B}_{(\rho)}$ with colors $1, \ldots, D$ respect

$$\omega(\mathcal{G}) \geq D\sum_{\rho}\omega(\mathcal{B}_{(\rho)}). \tag{A3}$$

The proof of this statement can be found in [42], lemma 7. The proof relies on the identification of the jackets of $\mathcal{B}_{(\rho)}$ as ribbon subgraphs of the jackets of $\mathcal{G}$.

Proposition 3.—If the degree of a $(D+1)$-colored graph $\mathcal{G}$ vanishes, i.e. all its jackets are planar, then $\mathcal{G}$ is dual to a D-sphere.

The proof of this lemma can be found in [40].

The graphs of degree 0 have been thoroughly analyzed in [41]. Their characterization relies on two lemmas.

Proposition 4.—If $D \geq 3$ and $\mathcal{G}$ is a $(D+1)$-colored graph with vanishing degree, then $\mathcal{G}$ has a face with exactly two vertices.

Proof.—All faces of $\mathcal{G}$ have an even number of vertices. Denote $|\mathcal{F}_s|$ the number of faces with $2s$ vertices. By Proposition 1 [taking into account that $\mathcal{G}$ has $(D+1)$ colors], the total number of faces of $\mathcal{G}$ is $|\mathcal{F}| = \sum_{s\geq 1}|\mathcal{F}_s| = (D[D-1]/2)p + D$. As a vertex belongs to $\frac{D(D+1)}{2}$ faces we have $\sum_{s\geq 1} s|\mathcal{F}_s| = (D[D-1]/2)p$. Eliminating $\mathcal{F}_2$ we get

$$\mathcal{F}_1 = 2D + \sum_{s\geq 3}(s-2)\mathcal{F}_s + \frac{D(D-3)}{2}p. \tag{A4}$$

The first two terms give a strictly positive contribution for any D, whereas the third term changes sign for $D = 3$. Thus $\mathcal{F}_1 \geq 1$ only for $D \geq 3$.

The fact that this proposition fails in $D = 2$ is the source of the difference between the large N limit of matrix models, dominated by planar graphs, and the large N limit of tensors of rank D, dominated by *melonic* graphs, which we describe below.

Proposition 5.—If $D \geq 3$ and $\mathcal{G}$ is a $(D+1)$-colored graph of vanishing degree, then it contains two vertices v and $\bar{v}$ separated by exactly D lines.

The proof of this lemma can be found in [41]. It relies on Proposition 4, but as it is somewhat convoluted we do not reproduce it here.

We exploit this lemma in the following way. Starting from a $(D+1)$-colored graph $\mathcal{G}$ we identify two vertices v and $\bar{v}$ separated by D lines. Erasing this subgraph and reconnecting its external lines we obtain a graph having two less vertices and degree 0 (as it can be checked explicitly). Iterating this erasing procedure we necessarily end up with a $(D+1)$-dipole, that is the graph having two vertices connected by $D+1$ lines. Conversely, every melonic graph can then be obtained by starting from the $(D+1)$-dipole and inserting such subgraphs (consisting in two vertices connected by D lines) arbitrarily on all the lines.

[1] P. Di Francesco, P. H. Ginsparg, and J. Zinn-Justin, Phys. Rep. **254**, 1 (1995).
[2] V. A. Kazakov, Phys. Lett. B **150**, 282 (1985).
[3] F. David, Nucl. Phys. B **257**, 543 (1985).
[4] T. Konopka, F. Markopoulou, and S. Severini, Phys. Rev. D **77**, 104029 (2008).
[5] V. A. Kazakov, Phys. Lett. A **119**, 140 (1986).
[6] D. V. Boulatov and V. A. Kazakov, Phys. Lett. B **186**, 379 (1987).
[7] E. Brezin, M. R. Douglas, V. Kazakov, and S. H. Shenker, Phys. Lett. B **237**, 43 (1990).
[8] V. A. Kazakov, Mod. Phys. Lett. A **4**, 2125 (1989).
[9] V. G. Knizhnik, A. M. Polyakov, and A. B. Zamolodchikov, Mod. Phys. Lett. A **3**, 819 (1988).
[10] F. David, Mod. Phys. Lett. A **3**, 1651 (1988).
[11] J. Distler and H. Kawai, Nucl. Phys. B **321**, 509 (1989).
[12] B. Duplantier, in *Les Houches, Session LXXXIII, 2005, Mathematical Statistical*, edited by A. Bovier, F. Dunlop,

F. den Hollander, A. van Enter, and J. Dalibard (Elsevier, New York, 2006), pp. 101–217.
[13] H. Grosse and R. Wulkenhaar, Commun. Math. Phys. **256**, 305 (2005).
[14] M. Disertori, R. Gurau, J. Magnen, and V. Rivasseau, Phys. Lett. B **649**, 95 (2007).
[15] V. Rivasseau, J. High Energy Phys. 09 (2007) 008.
[16] V. Rivasseau and Z. Wang, arXiv:1003.1037.
[17] Z. Wang, arXiv:1104.3750.
[18] G. 't Hooft, Nucl. Phys. B **72**, 461 (1974).
[19] E. Brezin and V. A. Kazakov, Phys. Lett. B **236**, 144 (1990).
[20] M. R. Douglas and S. H. Shenker, Nucl. Phys. B **335**, 635 (1990).
[21] D. J. Gross and A. A. Migdal, Phys. Rev. Lett. **64**, 127 (1990).
[22] E. Brezin, C. Itzykson, G. Parisi, and J. B. Zuber, Commun. Math. Phys. **59**, 35 (1978).
[23] W. Tutte, Can. J. Math. **15**, 249 (1963).
[24] G. Schaeffer, Electron. J. Comb. **4**, R20 (1997).
[25] M. Bousquet-Mélou and G. Schaeffer, Adv. Appl. Math. **24**, 337 (2000).
[26] V. Rivasseau, F. Vignes-Tourneret, and R. Wulkenhaar, Commun. Math. Phys. **262**, 565 (2006).
[27] R. Gurau, J. Magnen, V. Rivasseau, and F. Vignes-Tourneret, Commun. Math. Phys. **267**, 515 (2006).
[28] J. Ambjorn, B. Durhuus, and T. Jonsson, Mod. Phys. Lett. A **6**, 1133 (1991).
[29] N. Sasakura, Mod. Phys. Lett. A **6**, 2613 (1991).
[30] M. Gross, Nucl. Phys. B, Proc. Suppl. **25**, 144 (1992).
[31] N. Sasakura, arXiv:1104.1463.
[32] N. Sasakura, Int. J. Mod. Phys. A **26**, 3249 (2011).
[33] N. Sasakura, Int. J. Mod. Phys. A **26**, 4203 (2011).
[34] R. Gurau, Commun. Math. Phys. **304**, 69 (2011).
[35] R. Gurau, Ann. Henri Poincare **11**, 565 (2010).
[36] R. Gurau, Classical Quantum Gravity **27**, 235023 (2010).
[37] P. Di Francesco, Nucl. Phys. B **648**, 461 (2003).
[38] R. Gurau, Ann. Henri Poincare **12**, 829 (2011).
[39] R. Gurau and V. Rivasseau, Europhys. Lett. **95**, 50004 (2011).
[40] R. Gurau, Ann. Henri Poincare **13**, 399 (2012).
[41] V. Bonzom, R. Gurau, A. Riello, and V. Rivasseau, Nucl. Phys. B **853**, 174 (2011).
[42] R. Gurau, Nucl. Phys. B **852**, 592 (2011).
[43] R. Gurau and J. P. Ryan, arXiv:1109.4812.
[44] J. B. Geloun, J. Magnen, and V. Rivasseau, Eur. Phys. J. C **70**, 1119 (2010).
[45] A. Baratin, F. Girelli, and D. Oriti, Phys. Rev. D **83**, 104051 (2011).
[46] J. Ben Geloun and V. Bonzom, Int. J. Theor. Phys. **50**, 2819 (2011).
[47] V. Bonzom and M. Smerlak, Ann. Henri Poincare **13**, 185 (2012).
[48] V. Bonzom, arXiv:1201.1931.
[49] J. P. Ryan, Phys. Rev. D **85**, 024010 (2012).
[50] S. Carrozza and D. Oriti, Phys. Rev. D **85**, 044004 (2012).
[51] V. Bonzom, R. Gurau, and V. Rivasseau, arXiv:1108.6269.
[52] D. Benedetti and R. Gurau, Nucl. Phys. B **855**, 420 (2012).
[53] R. Gurau, Phys. Rev. D **84**, 124051 (2011).
[54] S.-J. Rey and F. Sugino, arXiv:1002.4636.
[55] J. Ambjorn, B. Durhuus, and T. Jonsson, Phys. Lett. B **244**, 403 (1990).
[56] R. Gurau, arXiv:1111.0519.
[57] J. Magnen, K. Noui, V. Rivasseau, and M. Smerlak, Classical Quantum Gravity **26**, 185012 (2009).
[58] D. Oriti, in *Foundations of Space and Time: Reflections on Quantum Gravity*, edited by G. Ellis, J. Murugan, and A. Weltman (Cambridge University Press, Cambridge, 2012).
[59] J. Ben Geloun and V. Rivasseau, arXiv:1111.4997.
[60] J. Ben Geloun and D. O. Samary, arXiv:1201.0176.
[61] V. Rivasseau, arXiv:1112.5104.
[62] F. Caravelli, arXiv:1012.4087.